Ethiopian Journal of Science and Sustainable Development

e-ISSN 2663-3205 *Volume 12 (2), 2025*

Journal Home Page: www.ejssd.astu.edu.et

Research Paper

Optimization of Performance and Emissions of RCCI Engine at Various Speed Conditions Using Response Surface Methodology Technique

Negasa Tesfaye Tefera*, Ramesh Babu Nallamothu, Getachew Alemayehu

Department of Mechanical Engineering, Adama Science and Technology University, P.O. Box 1888, Adama, Ethiopia

Article Info

Article History:
Received 22 May 2025
Received in revised form 22 July 2025
Accepted 23 July 2025

Keywords:
Biodiesel,
combustion efficiency,
dual-fuel,
emission,
n-butanol

Abstract

The demand for reduction of greenhouse gases and the implementation of stringent emission regulations have compelled researchers and engine makers to look for alternative approaches of increasing efficiency from the internal combustion engine. This study investigated the optimization of performance and emission characteristics of a reactivity-controlled compression ignition (RCCI) engine. A dual-fuel strategy was introduced by employing gasoline/n-butanol blends (G25n-b75, G50n-b50, and G75n-b25) as low reactivity fuels and a biodiesel blend (B20) as a high reactivity fuel. Experiments were carried out on a single-cylinder, water-cooled compression ignition engine under varying engine speeds (2400, 2600, and 2800 rpm). Response Surface Methodology (RSM) was used to evaluate the effects of engine speed and fuel blend ratio on brake torque (BT), brake power (BP), brake specific fuel consumption (BSFC), nitrogen oxides (NOx), hydrocarbons (HC), carbon dioxide (CO_2), and carbon monoxide (CO). The optimal operating condition was found at engine speed of 2557 rpm with a 47% n-butanol blend ratio, resulting in improved performance and reduced emissions, with BT, BP, BSFC, NOx, HC, CO_2 and CO values of 14.86 Nm, 4.04 kW, 0.379 kg/kWh, 102 ppm, 32 ppm, 4.63%, and 0.87%, respectively. Analysis of Variance confirmed the statistical significance of the model with high R^2 values: BT (97.98%), BP (98.39%), BSFC (98.62%), CO_2 (94.72%), CO (98.89%), NOx (99.66%), and HC (97.14%). The findings demonstrated the synergistic potential of gasoline/n-butanol and biodiesel dual-fuel RCCI mode to enhance combustion efficiency and to reduce emissions, offering a viable alternative for sustainable engine operation.

1. Introduction

Compression ignition (CI) engines are known for their superior thermal efficiency and robust power output, which make them highly valuable across sectors such as transportation, agriculture, power generation, and construction engineering (Zhao et al., 2021). However, the conventional diesel engines must involve rapidly reducing emissions and improving thermal efficiency in response to escalating environmental concerns and the ongoing energy crisis (Ouchikh et al., 2022). Low-temperature combustion mode, including premixed charge compression ignition (PCCI) and homogeneous charge compression ignition (HCCI), can break the conventional trade-off association between nitrogen oxides (NOx) and particulate matter (PM), effectively avoiding the primary regions responsible for the formation of both pollutants (Liu et al., 2022). However, both PCCI and HCCI combustion modes are predominantly governed by chemical kinetics, meaning that variables such as pressure, temperature, and equivalency ratio strongly influence the combustion

*Corresponding author, e-mail: negasa.tesfaye@astu.edu.et

https://doi.org/10.20372/ejssdastu:v12.i2.2025.1082

phase and rate of heat release, making precise control difficult (Zhang et al., 2023). At high loads, these modes face a limited working range due to an excessive rate of pressure rise. In contrast, at low loads, they often suffer from elevated hydrocarbons (HC) and carbon monoxide (CO) emissions due to lower combustion temperatures (Chaudhari & Deshmukh, 2019).

A more advanced strategy, known as reactivity-controlled compression ignition (RCCI), has been introduced to address these limitations and enable better combustion control, particularly under high load conditions (Habtamu et al., 2023b). In the RCCI engine, the utilization of low reactivity fuel (LRF) in conjunction with high reactivity fuel (HRF) serves to effectively regulate the timing of the combustion phase (Habtamu et al., 2024). These fuels are mixed in the combustion chamber to enhance self-ignition characteristics (Jagankumar et al., 2020). RCCI can be applied under high load conditions using both single and multiple injection strategies, allowing the engine to benefit from features of both compression ignition and spark ignition (Shim et al., 2020). In this configuration, volatile LRFs, such as alcohols and gasoline, are supplied into the intake manifold through the port fuel injection (PFI), while HRFs, such as biodiesel and diesel, are supplied directly into the cylinder through in-cylinder direct injection (DI) (Zheng et al., 2018). By varying the ratio of LRF to HRF, the reactivity of the fuel mixture can be adjusted, enabling control over the combustion phase under different load conditions. Compared to HCCI and PCCI methods, the RCCI offers enhanced precision in managing both ignition and combustion (Vijai et al., 2025).

Within the RCCI approach, biodiesel (Mali et al., 2024) and diesel (Habtamu et al., 2023a) are most commonly used as HRFs. Biodiesel is typically defined as the ethyl or methyl esters of fatty acids derived from plant (vegetable) oils and animal fats, and it exhibits properties that make it a substitute for diesel fuel in CI engines (Negasa et al., 2025b). Trans-esterification is the most commonly used method for biodiesel production. In this process, triglycerides react with short-chain alcohols to produce biodiesel as the main product, with glycerol formed as a by-product (Yohannes et al., 2024). For port injection in RCCI engines, LRFs, such as gasoline (Saxena & Maurya, 2020), natural gas (Kakoee et al., 2018), n-butanol (Zhao et al., 2021), methanol (Jia & Denbratt, 2018), ethanol (Ramachandran & Subramanyan 2024), and hydrogen (Kumar & Paul, 2023), have been investigated. Among these, n-butanol offers distinct advantages over ethanol and methanol, including a higher flash point and lower vapor pressure, which improves handling safety (Jin et al., 2019). It also exhibits lower corrosiveness, extending fuel system lifespan, and it has a higher cetane number than ethanol and methanol, making it less prone to misfires in low-temperature combustion modes, such as HCCI, PCCI, and RCCI (Wang et al., 2021a).

Cottonseed oil (CSO) is considered a promising feedstock for this study due to its high yield, low cost, and widespread availability in Ethiopia**.** Cotton seeds typically has oil content ranging from 17 to 25% (Singh et al., 2019). When cottonseed oil-based biodiesel are used as the HRF, it offers favorable properties such as high cetane number, good oxidative stability, and a sustainable production route; these make it a promising alternative to conventional diesel in dual-fuel RCCI systems (Negasa et al., 2025a).

Several studies have explored RCCI engines using alcohols and hydrogen as LRFs and biodiesel blends as HRF. Zheng et al. (2018) investigated the effects of alcohols and biodiesel on RCCI engine and reported a significant simultaneous reduction in both soot and NOx emissions. Okcu et al. (2021) evaluated the impacts of isopropanol-butanol-ethanol on the emission of an RCCI engine, revealing a reduction in both soot and NOx emissions. Ganesh et al. (2019) explored iso-butanol/diesel on RCCI combustion in a non-road CI engine and found that the iso-butanol/diesel blend led to a simultaneous increase in brake thermal efficiency (BTE), along with lower NOx and soot emissions. Wang et al. (2019) compared the effects of gasoline/diesel and gasoline/polyoxymethylene dimethyl ethers (PODE) on RCCI and found that stable and manageable RCCI operation is attainable with PODE. Additionally, using PODE can result in enhanced indicated thermal efficiency and significantly reduced soot emissions. Wategave et al. (2025) investigated the performance and emission behavior of a RCCI engine fueled with 20% Juliflora biodiesel–diesel blend as HRF and ethanol as LRF, under varying loads (0–100%), LRF ratios (30–

60%), and with Exhaust Gas Recirculation. Engine parameters such as BTE, Brake-specific fuel consumption (BSFC), cylinder pressure (CP), heat release rate (HRR), and emissions (HC, CO, NOx, and smoke opacity (SO)) were evaluated and optimized using a hybrid Deep Belief Network–Aquila Optimization method, achieving a high regression coefficient of 0.99961. Optimal engine operation was found at 80% load, 60% LRF, and 15% exhaust gas recirculation (EGR), with confirmatory error analysis showing improvements in efficiency and emission reductions, particularly in NOx, CO, and SO. Deb et al. (2025) explored the effects of HRF injection advancement and hydrogen–biodiesel premix ratio on the performance, combustion, and emissions of an RCCI engine. Advancing the HRF injection angle up to 70°bTDC and increasing the hydrogen premix ratio to 60% improved combustion stability and allowed for higher LRF usage without compromising engine performance. At a 50% hydrogen premix and 70°bTDC injection timing, brake thermal efficiency improved by 15%, while NOx, soot, CO, and unburned hydrocarbons (UHC) emissions were reduced by 73, 85, 61, and 42%, respectively, compared to conventional diesel combustion. Ramachandran & Subramanyan (2024) modified a CI engine to operate in RCCI mode using hydrogen-enriched compressed natural gas (HCNG) and hydrogen (H_2) as LRFs with a diesel–karanja biodiesel blend (BD20) as the pilot fuel. Optimal combustion and emissions performance were achieved with 75–80% energy share (ES) for HCNG and 30–40% for H_2, resulting in reduced combustion noise and cleaner emissions. At optimal conditions, HC emissions were 42 ppm for H_2 and 138 ppm for HCNG, while CO emissions dropped to 0.02–0.04% at higher LRF energy shares.

Due to the substantial time and financial investment required to optimize input factors such as engine load, speed, and fuel blend, there has been a recent increase in interest in alternative analytical and statistical methods (Elumalai & Ravi, 2022). To minimize the number of engine tests, a variety of optimization methods, such as Taguchi, artificial neural network, response surface methodology (RSM), Genetic algorithm, were applied to identify an engine's operating parameters (Ramachandran et al., 2023). Among these methods, RSM is recognized as a powerful statistical process optimization tool that aids in identifying optimal conditions within multi-variable systems. It integrates a blend of statistical and mathematical techniques for the purposes of process modeling and analysis. In comparison to alternative methods, RSM presents a relatively straightforward implementation, necessitates fewer computational resources than artificial neural network, or genetic algorithm, and offers an interpretable regression model that elucidates both individual and interaction effects of the variables (Rajavel et al., 2025). While Taguchi primarily emphasizes robustness and signal-to-noise ratios, RSM is more adept at developing predictive models and investigating response surfaces, rendering it the preferred choice for this study, where establishing a clear mathematical relationship between variables and outputs is crucial (Manojkumar et al., 2022).

Despite substantial research on RCCI engines, there remains a notable gap in the literature regarding the combined use of n-butanol/gasoline blends as LRF and biodiesel blend as HRF under varying engine speeds. Previous studies have often employed pure gasoline or pure n-butanol as LRF in dual-fuel RCCI operation. However, pure gasoline, while readily available, exhibits low oxygen content and poor auto ignition characteristics, leading to incomplete combustion and higher CO and HC emissions (Elbanna et al., 2022). Conversely, pure n-butanol, through oxygenated and renewable, suffers from high latent heat of vaporization and low volatility, which can result in delayed combustion and reduced brake thermal efficiency (Mahla et al., 2023).

Thus, the present study addressed the identified research gaps by using RSM with a central composite design (CCD) to explore the combined effects of engine speed and n-butanol/gasoline blend ratio on the performance and emission characteristics of an RCCI engine. This approach enabled the development of accurate regression models and the identification of optimal operating conditions for improved efficiency and reduced emissions when using renewable fuel combinations. Hence, the main objective of this study was to optimize engine speed and fuel blend ratio in an RCCI engine using RSM so as to enhance performance while minimizing harmful emissions.

2. Materials and Methods

2.1 Biodiesel production

The CSO biodiesel was synthesized using the conventional transesterification process in the Chemistry Laboratory of the Department of Chemistry at Adama Science and Technology University (Adama, Ethiopia). The transesterification process was employed to convert CSO into biodiesel, which significantly reduces its viscosity. One of the most critical factors in selecting the transesterification process is the free fatty acid (FFA) content. The FFA content should be less than 1% to proceed with base-catalyzed transesterification (Hayyan et al., 2011). In this study, the FFA content of CSO was found to be below 1%, making it suitable for this process. In this method, a measured quantity of CSO was placed in a beaker and preheated to 60 °C. Methanol and Potassium Hydroxide (KOH) catalysts were mixed to prepare a potassium methoxide (CH_3KO) solution, which was then added to the preheated oil. The mixture was agitated consistently at a uniform rate of 500 rpm for the entire duration of the reaction. The reaction temperature of the process was set at a constant temperature of 60ºC since methanol has a boiling point of 64.7 °C. The transesterification reaction was carried out with a methanol-to-KOH weight ratio of 15:1, a methanol-to-oil ratio of 1:6, and a reaction time of 52 min. Once the transesterification reaction was finished, the products were transferred to a separating funnel and allowed to settle for 24 h. After extracting the crude glycerol from the methyl ester, the product was repeatedly washed and heated to 130 °C for one hour to remove water and the leftover residue.

2.2 Experimental setup

The experiments were conducted on the CI engine, which was modified into an RCCI engine by integrating a PI injection system, governed by an Arduino board microcontroller. The engine test rig was connected with a data acquisition system that included an AC dynamometer, which was directly connected to the output shaft of the engine. This setup is located at Jimma Institute of Technology, with a more complete representation provided in Figure 1. Overall, a single-cylinder diesel engine was adapted to function in RCCI engine mode, utilizing a biodiesel-diesel blend as HRF and a gasoline/n-butanol blend as the LRF. The LRF was mainly introduced into the air intake stream, creating a low reactivity charge premixed that was delivered to the engine cylinder. Meanwhile, the HRF was directly supplied into the cylinder towards the conclusion of the compression stroke. The ignition of the injected HRF occurred through the combustion of the premixed mixture of LRF and air.

The comprehensive fundamental specifications of the engine are presented in Table 1. Gasoline, diesel, n-butanol, and biodiesel fuels that met quality standards were used in this study. The physicochemical properties of gasoline, biodiesel, and diesel (Table 2) were experimentally measured as part of this study. However, the properties of n-butanol were sourced from the literature. Based on previous researchers (Fırat et al., 2022; Ramachandran & Subramanyan, 2024; Zarrinkolah & Hosseini, 2022) the HRF, constant B20 (80% diesel and 20% biodiesel blend) was fixed and delivered directly into the engine cylinder via direct injection; while LRF, a gasoline/n-butanol blend, was injected into the intake manifold utilizing port fuel injection. B20 was fixed based on the recommendation of ASTM; approved B20 blends meet modern fuel specifications (ASTM D7467), and diesel OEMs widely endorse the use of B20 without modifications.

Table 1: Comprehensive specifications of the test engine

Type of engine	Compression-ignition
Company, Model	GUNT, CT110
No. of cylinders	1
No. of strokes	4
Air intake type	Naturally aspirated
Compression ratio	23:1
Bore *Stroke	75mm *70 mm
Output power @3000 rpm	7.5 kW
Cooling system	Water-cooled

An electronic fuel pump was employed to supply the gasoline/n-butanol blend to the port fuel injector, with the injection volume controlled by a programmed Arduino board microcontroller. Experiments were carried out at constant engine load and constant injection timing while varying engine speeds and blended fuel ratios.

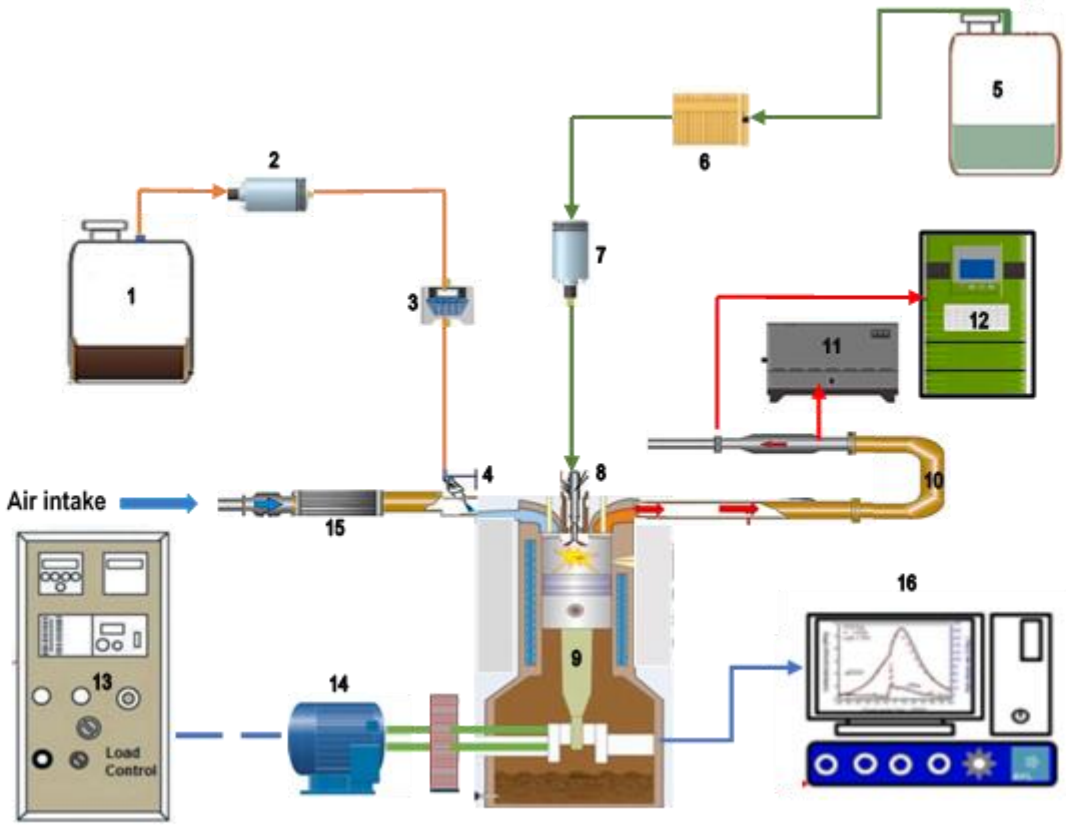

1	Fuel tank for LRF	**2**	Electronic fuel pump	**3**	Arduino microcontroller
4	Port injector	**5**	Fuel tank for HRF	**6**	Fuel filter
7	High-pressure fuel pump	**8**	Direct injector	**9**	Test Engine
10	Exhaust manifold	**11**	NOx gas analyzer	**12**	Exhaust emissions analyzer
13	Control panel	**14**	Dynamometer	**15**	Air filter
16	Data acquisition				

Figure 1: Schematic diagram of the experimental setup

Table 2: Physicochemical properties of fuels

Parameter	Diesel	Gasoline	n-butanol (Wang et al., 2021b)	B100
Density @15°C (kg/m^3)	840.00	720.0	810.00	880.00
Kinematic viscosity @40°C (mm^2/s)	3.15	0.7	2.22	4.41
Flash point (°C)	69.00	-43.0	35.00	178.00
Cetane number	52.00	13.0	17-25	53.10
Auto ignition temperature (°C)	210.00	300.0	342.70	-
Low heating value (MJ/kg)	42.50	42.4	33.80	41.42

In all the experiments, the start of injection timing for biodiesel-diesel blend fuel was consistently set at 14°CA BTDC, based on the manufacturer's original engine design specifications. This timing was selected to maintain consistency with standard operating conditions for the baseline diesel engine. The premixed fuel ratio (r_p) is generally defined as the proportion of energy supplied through port fuel injection (PFI) to the total energy input from both direct injection (DI) and PFI, as expressed by Eq. (1) (Pedrozo et al., 2022).

$$r_p = \frac{m \times LHV_{G-nb}}{M \times LHV_{B20} + m \times LHV_{G-nb}} \quad (1)$$

where: *m* is the mass flow rates of LRF, *LHV* is the lower heating value fuel, and *M* is the mass flow rates of HRF. The subscript B20 is 80% of diesel fuel and 20% of biodiesel and G-nb for the gasoline/n-butanol blend.

2.3 Experimental design

The RSM combines statistical and mathematical techniques to analyze engineering problems and develop models where multiple dependent (output) variables are influenced by independent (input) factors. The main goals of this work were to optimize RCCI engine operating conditions and create a predicted model while conserving resources, effort, and time. The design matrix was developed using CCD and the tests were performed according to this matrix. The data needed for RSM analysis was gathered from laboratory experiments following a design matrix generated by Minitab 20.3 software. In this study, two input (independent) variables, namely, engine speed (A) and ratio of n-butanol/gasoline blend (B) were chosen to examine their effects on output (dependent) variables, which are engine performance and emissions parameters. To evaluate the reliability and statistical significance of the developed models for each response variable, Analysis of variance (ANOVA) was performed. The engine speed (A) of 2400, 2600, and 2800 rpm were deliberately selected to investigate the engine's performance and emission behavior under high, yet sub-maximal operating conditions, just below the rated speed of 3000 rpm. This approach ensures safe and stable engine operation during testing while capturing meaningful variations in combustion and emissions. The n-butanol PFI ratio (B) of 25, 50 and 75 were considered as low, medium and high, respectively.

Eq. (2) illustrates the quadratic model used to derive the responses based on the factors.

$$Y = X_0 + \sum_{i=1}^{k} X_i A_i + \sum_{i=1}^{k} X_{ii} B^2 i + \sum_{j=i+1}^{k} . \sum_{i=1}^{k} X_{ij} C_{ij} \quad (2)$$

where Y is the response variable; A_i, B_i, and C_i are the input factors; X_0 and X_i represent intercept and first-order regression coefficient, respectively; k is the total number of process factors and X_{ii} is the quadratic regression coefficient.

2.4 Experimental uncertainty analysis

Experimental investigations are inherently influenced by uncertainty arising from various factors, including human error, the state of measuring devices, methods of data collection, and fluctuating environmental conditions. The precision of measurements is vital for obtaining reliable study results. In this study, to limit the errors calibration of the measuring apparatus employed was carried out. To enhance the accuracy of the analysis, three readings were recorded and averaged, thereby minimizing potential measurement discrepancies. The total uncertainty associated with the engine output variables was calculated utilizing the root-mean-square method. The overall uncertainty of the experiment was determined by using Eq. (3) (Jatoth et al., 2021). Based on the uncertainty values of the variables (Table 3) and equation (3), the overall uncertainty is found to be 2.77%.

$$\Delta U = \sqrt{\left\{\left(\frac{\partial U}{\partial X_1} \Delta X_1\right)^2 + \left(\frac{\partial U}{\partial X_2} \Delta X_2\right)^2 + . . . + \left(\frac{\partial U}{\partial X_n} \Delta X_n\right)^2\right\}} \quad (3)$$

Simply, $\Delta U = \sqrt{\{(BT)^2 + (BP)^2 + (BSFC)^2 + (NOx)^2 + (CO)^2 + (CO_2)^2 + (HC)^2\}}$

Table 3: Uncertainty of the responses

Parameter	Accuracy (%)	Uncertainty (%)
BP (kW)	±0.10	±0.84
BT (Nm)	±0.20	±0.90
BSFC (kg/kWh)	±0.05	±1.12
CO (%vol.)	±0.06	±1.03
CO_2 (%vol.)	±0.10	±0.95
HC (ppm)	±3.00	±1.06
NOx (ppm)	±12.00	±1.34

3. Results and Discussion

3.1 Model analysis of response surface methodology

The foundation for a total of 13 experimental runs was established through a design matrix developed using the CCD of RSM, focusing on the two primary factors: speed (A) and the ratio of n-butanol to gasoline blend (B). The study intended to analyze the individual and interactive effects of these factors on the performance and emissions of an RCCI engine. A quadratic polynomial model was utilized to define the numerical correlation between the output factors and the process factors. Furthermore, a mathematical formulation was established to conduct multiple regression analysis, which facilitated the creation of predictive models, as indicated in Eq. (4-10).

To evaluate the correlations and ascertain the impact of the input variables on the response variables, the statistical technique of ANOVA was employed. Table 4 illustrates the input and output along with the experimental runs organized in a design matrix.

The assessment of the model's quality was conducted through various statistical parameters: F-value, P-value, R^2, and Adj-R^2. A favorable model fit is suggested by a higher Adj-R^2 value that is in close proximity to the R^2, particularly when the R^2 approaches 1. The outcomes of the experiments can be contrasted to anticipated models using R^2. The R^2 for BT, BP, BSFC, CO_2, CO, NOx, and HC were 97.98, 98.39, 98.62, 94.72, 98.89, 99.66 and 97.14%, respectively. These values, which are extremely close to 1, reflect a high level of accuracy when compared to analytical results.

$$BT\ (Nm) = 4.92 - 0.00693A + 0.0658B - 0.00001A^2 - 0.000523B^2 - 0.000007AB \quad (4)$$

$$BP\ (kW) = 0.71 + 0.00161A + 0.01055B - 0.00000001A^2 - 0.000121B^2 - 0.0000001AB \quad (5)$$

$$BSFC\ (kg/kWh) = 0.304 + 0.00015A - 0.000859B - 0.0000001A^2 - 0.000001B^2 - 0.0000001AB \quad (6)$$

$$CO_2\ (vol.) = 31.32 - 0.02028A - 0.0853B + 0.000004A^2 + 0.0000542B^2 + 0.00001AB \quad (7)$$

$$CO\ (vol.) = 0.99 - 0.000795A - 0.00526B + 0.0000001A^2 + 0.000069B^2 + 0.000001AB \quad (8)$$

$$HC = 233 - 0.165A - 0.647B + 0.000038A^2 + 0.01086B^2 - 0.0002AB \quad (9)$$

$$NOx = 1165 - 1.307A - 2.679B + 0.000278A^2 + 0.00611B^2 + 0.0006AB \quad (10)$$

Table 4: Experimental matrix of RSM with the results of the responses

Run	Factors		Output Responses						
	A	B	BT	BP	BSFC	CO_2	NOx	CO	HC
1	2600	50	14.83	4.08	0.350	5.3	108	0.902	33
2	2600	85	14.01	3.78	0.392	5.6	96	0.960	44
3	2600	50	14.81	4.07	0.352	5.2	107	0.903	32
4	2600	15	14.34	4.04	0.365	4.6	131	1.017	47
5	2800	25	14.46	4.20	0.341	5.4	169	1.158	51
6	2600	50	14.85	4.06	0.354	5.2	106	0.904	34
7	2317	50	14.79	3.80	0.398	4.9	81	0.715	28
8	2800	75	14.15	4.09	0.371	5.2	150	1.133	43
9	2600	50	14.84	4.06	0.351	5.4	108	0.905	33
10	2400	75	14.51	3.79	0.401	4.4	74	0.771	35
11	2883	50	14.65	4.30	0.351	5.7	175	1.141	42
12	2400	25	14.68	3.89	0.381	4.8	105	0.779	39
13	2600	50	14.82	4.07	0.352	5.2	109	0.902	32

The model's significance can be ascertained through the P-value. For a given model, a P-value < 0.05 shows statistically significance, indicating a divergence from the null hypothesis. Conversely, P-values exceeding 0.05 imply that the model lacks significance. Additionally, the ANOVA results revealed higher F-values, further supporting the significance of the model. The findings of the ANOVA for BP, BSFC, and BT are presented in Table 5, whereas Table 6 illustrates the ANOVA results related to the emission characteristics. Table 7 presents additional diagnostic parameters utilized for evaluating the constructed response variable model. The R^2 reflects both the accuracy and adequacy of the model. Furthermore, the disparity between the adj-R^2 and pred-R^2 values serves as an indicator of the model's consistency. The variability in data is demonstrated by the values of standard deviation (Std. Dev).

Table 5: ANOVA for engine performance

Source	BT		BP		BSFC	
	P-value	F-value	P-value	F-value	P-value	F-value
Model	0.0001	68.04	0.0001	323.77	0.0001	99.86
A-Speed	0.0010	27.47	0.0001	1413.37	0.0001	346.62
B- n-butanol ratio	0.0001	40.68	0.0001	194.74	0.0001	144.74
A^2	0.0290	7.47	0.5760	0.04	0.0810	4.40
B^2	0.0001	269.92	0.0001	10.15	1.0000	0.00
AB	0.2240	1.78	0.8550	0.04	0.0950	3.72

Table 6: ANOVA for engine emissions

Source	CO_2		CO		HC		NOx	
	P-value	F-value	P-value	F-value	P-value	F-value	P-value	F-value
Model	0.0001	25.13	0.0001	124.88	0.0001	47.52	0.0001	406.28
A	0.0001	51.75	0.0001	585.46	0.0001	84.24	0.0001	1646.27
B	0.0190	9.31	0.0800	4.19	0.0070	14.03	0.0001	218.78
A^2	0.0080	13.25	0.1270	3.00	0.0330	7.00	0.0001	152.26
B^2	0.0001	56.70	0.0010	33.61	0.0001	136.36	0.0040	18.59
AB	0.4270	0.71	0.6780	0.19	0.2330	1.70	0.0400	6.36

Table 7: Evaluation of ANOVA model

Parameter	BT	BP	BSFC	CO	CO_2	HC	NOx
Std. Dev	0.0525	0.0264	0.0026	0.0196	0.1187	1.5530	2.3780
R^2	0.9798	0.9839	0.9862	0.9889	0.9472	0.9714	0.9966
Adj-R^2	0.9654	0.9724	0.9763	0.9810	0.9095	0.9509	0.9941
Pred-R^2	0.8624	0.8909	0.9180	0.9213	0.6604	0.8235	0.9781

3.2 Performance analysis

3.2.1. Brake torque

The torque produced by the engine, evaluated at the crankshaft or input shaft while accounting for internal resistive forces such as friction, is referred to as brake torque (BT). The ANOVA analysis presented in Table 5, reveals that both A and B exert a considerable influence on the BT, with P-values of 0.001 and 0.0001, respectively, alongside notable F-values that suggest a significant effect. Furthermore, the term associated with B^2 demonstrates a high level of significance, with an F-value of 269.92 and a P-value of 0.0001. In contrast, the AB and A^2 terms appear to have a minimum impact on the overall response. The relationship between engine speed and n-butanol content on BT (Figure 2) illustrates BT to remain relatively stable across varying engine speeds, fluctuating between 14.01 and 14.85 Nm with no extreme deviations. This stability indicates that n-butanol ratios up to 50% have a minimum detrimental impact on the torque output at tested the engine speeds. At 2600 rpm and 50 % n-butanol, the BT achieved a peak of 14.85 Nm, illustrating the blend's ability to maintain strong combustion efficiency. However, as the n-butanol ratio increases up to 85.35 % at the same speed, BT drops to 14.01 Nm because of minimum calorific value of n-butanol**.**

3.2.2. Brake power

Brake power (BP) refers to the effective power output of an engine, which is quantified at the output shaft. This measurement accounts for the losses incurred due to friction and other internal components of the engine BP. It is evident from Table 5 that the BP is significantly influenced by A and B terms, with both showing highly significant P-values (0.0001) and F-values of 1413.37 and 194.74, respectively. The engine speed has the strongest impact on BP, as higher speeds generally enhance BP by allowing more fuel combustion per unit time, though excessively high speeds could reduce efficiency due to increased friction and incomplete combustion. The n-butanol ratio affects BP as the result of its lower calorific value compared to the conventional fuels, though its oxygen content can improve combustion efficiency. The term B^2 exhibits significance, proved by an F-value of 10.15 and a P-value of 0.0001. Conversely, the terms A^2 and AB seem to exert a minimum influence on the BP. The relationship between engine speed and the n-butanol ratio on BP is illustrated in Figure 3. The findings suggest that BP generally rises with increasing engine speed, specifically between 2317 rpm (3.80 kW) and 2883 rpm (4.30 kW). Additionally, as the n-butanol ratio increases, BP increases up to a certain point, then experiences a slight reduction due to the lower energy density of n-butanol; for instance, at 2800 rpm, BT drops from 4.20 kW at 25% of n-butanol to 4.09 kW at 75% n-butanol. The peak BP was achieved at 2883 rpm with 50% n-butanol content yielding a BP of 4.30 kW.

3.2.3. Brake specific energy consumption

Brake-specific energy consumption (BSFC) is a key engine parameter, defined as the amount of fuel consumed per unit of power generated over a specific period of time. This parameter is influenced by both the fuel's heating value and specific fuel consumption. The significance of this analysis becomes particularly evident when evaluating various fuels that possess distinct characteristics, including differing heating values and cetane number. The ANOVA results presented in Table 5 indicated that BSFC is notably affected by both A and B terms, underscoring their essential contributions to engine performance. Among these terms, A exerts the most substantial influence on BSFC, evidenced by a highly significant F-value of 346.62. The B term also plays a significant role in determining BSFC, with an F-value of 144.74, as an elevated ratio tends to raise fuel consumption as a result of the lower energy density of n-butanol. The quadratic term A^2 has negligible impact, while both quadratic term B^2 and interaction term AB are statistically insignificant. The interaction between engine speed and n-butanol ratio concerning BSFC is depicted in Figure 4. The plot shows that BSFC increases with higher n-butanol content due to lower energy density, necessitating a greater fuel volume to generate the same power output. Conversely, higher engine speeds result in reduced fuel consumption to sustain the desired power levels. The lowest BSFC of 0.351 kg/kWh was attained at 2883 rpm with a G50n-b50 blend.

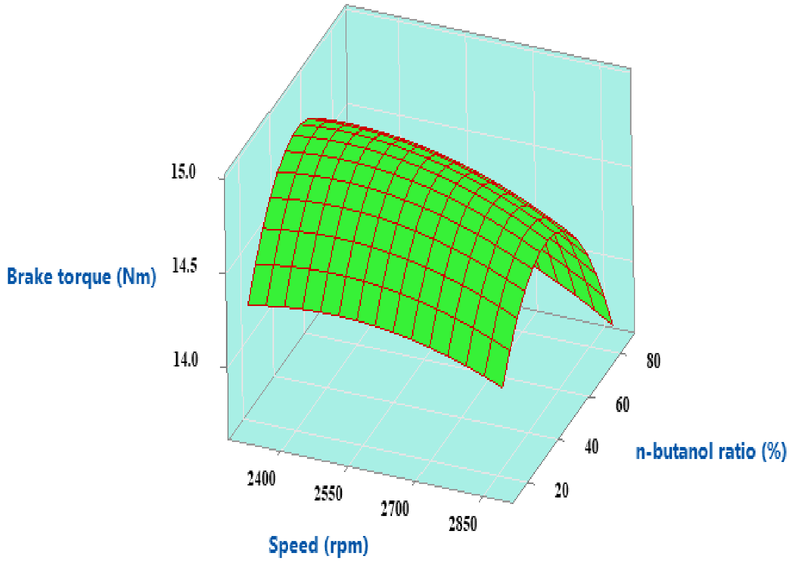

Figure 2: Surface plot of Brake torque vs engine speed and n-butanol ratio

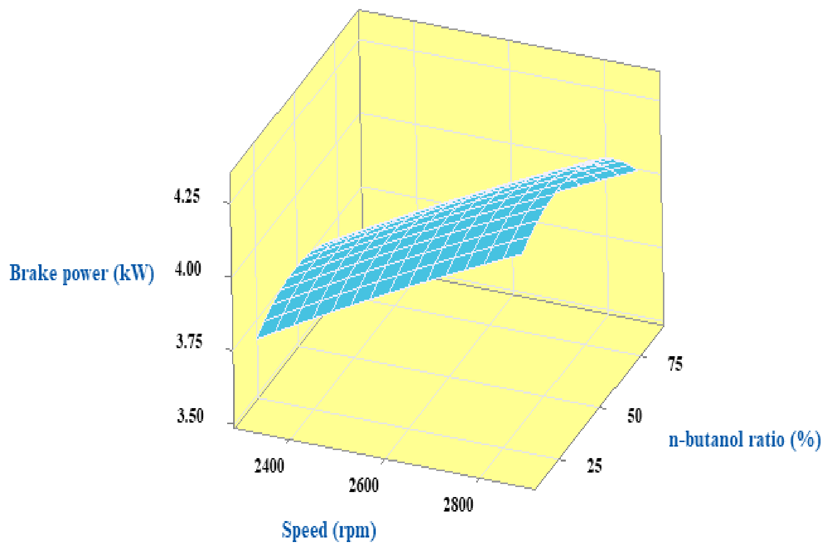

Figure 3: Brake power vs engine speed and n-butanol ratio surface plot

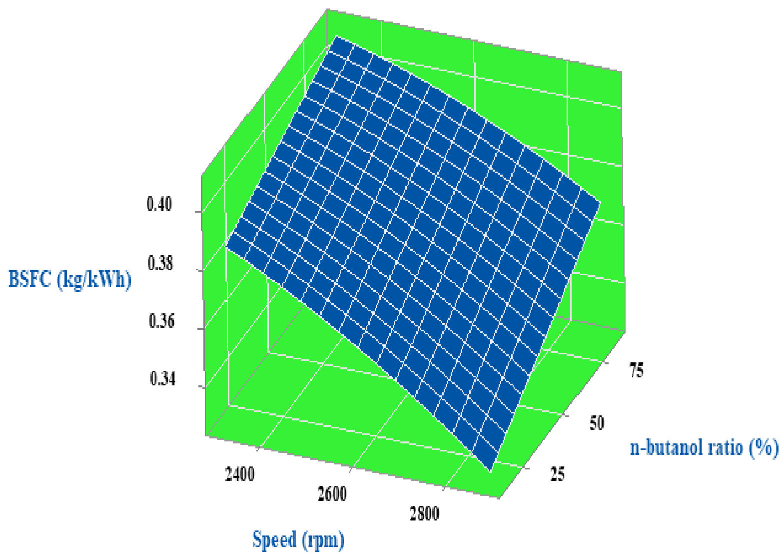

Figure 4: BSFC vs engine speed and n-butanol ratio surface plot

3.3 Emission analysis

3.3.1.Nitrogen oxides and carbon dioxide emissions

The ANOVA findings presented in Table 6 indicated that A and B terms play critical roles in influencing emissions of both NOx and CO_2. Specifically, the A term exerts a substantial impact on NOx with a highly significant F – value of 1646.47 and P – value of 0.0001. The B term also significantly affects NOx emission, F – value of 218.78 and a P-value of 0.0001. Additionally, the quadratic terms A^2 and B^2 are significant, due to an F-value of 152.26 and 18.59, respectively. In terms of CO_2 emission, both the A term (P-value = 0.0001, F-value = 51.75) and the B term (P-value = 0.019 and F-value = 9.31) are again found to have substantial effects. The interaction term AB shows a minor influence on both NOx and CO_2 emissions. Figure 5 depicts the synergistic effects of engine speed and n-butanol content on NOx emissions. It can be observed that NOx level rises with increasing engine speeds; however, at lower speeds, emissions of NOx are mitigated as a result of a decrease in combustion temperature. Figure 5 demonstrates that NOx decreases as the n-butanol content increases (for instance, at 2400 rpm, the NOx level reduced from 105 ppm at 25% of n-butanol to 74 ppm at 75% n-butanol). The lowest NOx emissions, attained at 2400 rpm with G25n-b75 was 74 ppm. The reduction in NOx emissions can be ascribed to the significant latent vaporization associated with the low reactivity of n-butanol fuel. This property leads to lower cylinder temperature, thereby diminishing the production of NOx emissions (Ganesan et al., 2020).

Additionally, Figure 6 illustrates the interaction between engine speed and the n-butanol content concerning CO_2 emission. It was observed that CO_2 emission rises with increasing speed; however, a high proportion of n-butanol leads to a reduction in emission. This reduction is likely attributable to the enhanced combustion efficiency provided by the oxygen content present in n-butanol. The lowest CO_2 emission level (4.4 %vol.) was attained at 2400 rpm with a G25n-b75 blend.

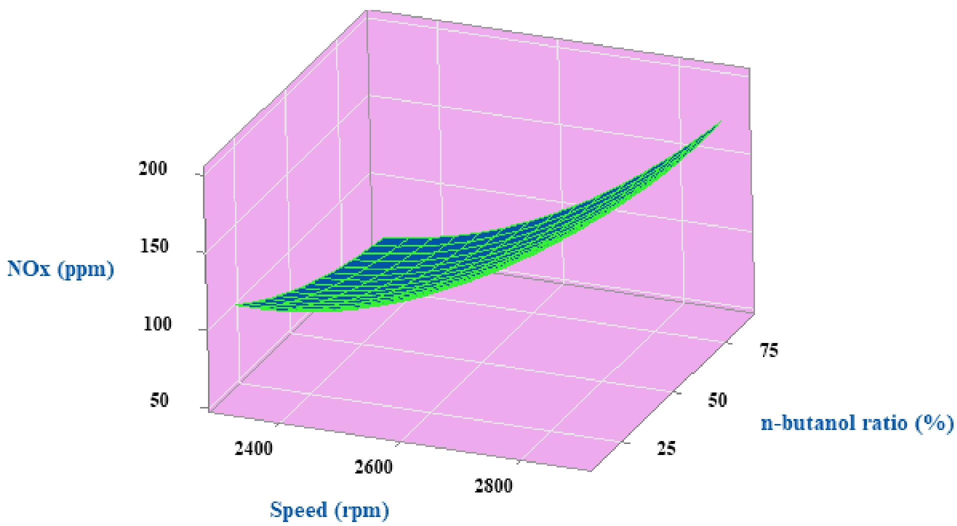

Figure 5: NOx vs engine speed and n-butanol ratio surface plot

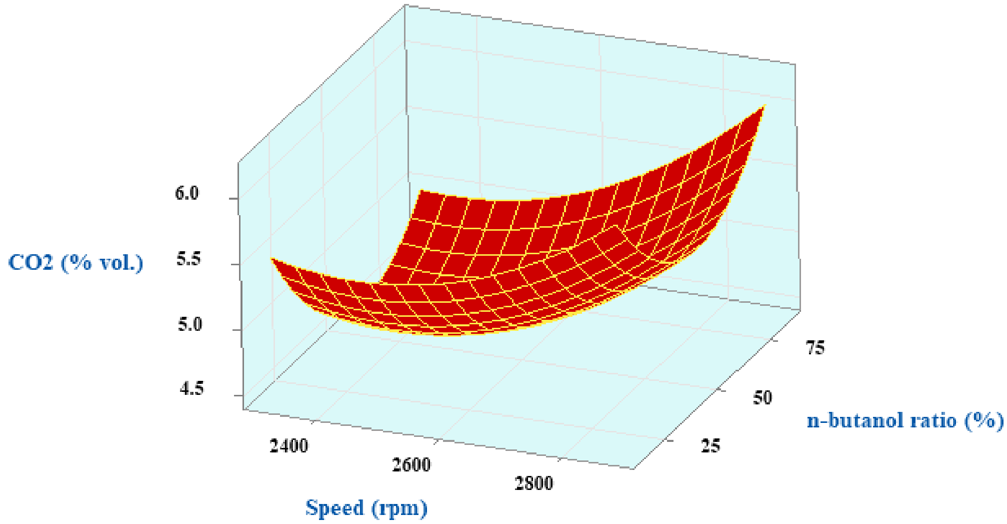

Figure 6: CO_2 vs engine speed and n-butanol ratio surface plot

3.3.2. Carbon monoxide and hydrocarbon emissions

The ANOVA analysis from Table 7 indicates that the A term has the most significant influence on both HC and CO emissions, with P-values of 0.0001 and an F-value of 82.42 for HC and 585.46 for CO, indicating strong linear effects. In contrast, the B term shows a moderate influence on HC emissions, with an F-value of 14.03 and a P-value of 0.007, while its effect on CO emission is less, reflected in a P-value (0.08) and an F-value (4.19). Notably, the quadratic term B^2 is more significant for HC, as shown by a P-value of 0.0001 and an F-value of 136.36, compared to CO, which has P-value of 0.001 and an F-value of 33.61. Analysis of Figures 7 and 8 reveal that both HC and CO emissions are at their lowest at minimum engine speeds; however, they increase significantly at higher speeds (for instance, CO emission rise from 0.715%vol. at 2317 rpm to 1.158% at 2800 rpm; while HC emissions increase from 28 ppm to 51 ppm). This trend indicates a tendency towards incomplete combustion at higher speeds. Furthermore, figures show a decrease in both CO and HC with enhancing levels of n-butanol up to certain point, then further increase of n-butanol increases both emissions (e.g., CO emission decrease from 0.779 % at 25% of n-butanol to 0.771 % at 75% of n-butanol; HC emissions decline from 39 ppm at 25% of n-butanol to 35 ppm at 35% of n-butanol). This reduction can be attributed to the enhanced oxygen content in n-butanol, which facilitates better combustion. The lowest CO and HC emissions were attained at a speed of 2317 rpm and a fuel blend of G50n-b50, resulting in an emission of 0.715 %vol. for CO and 28 ppm for HC.

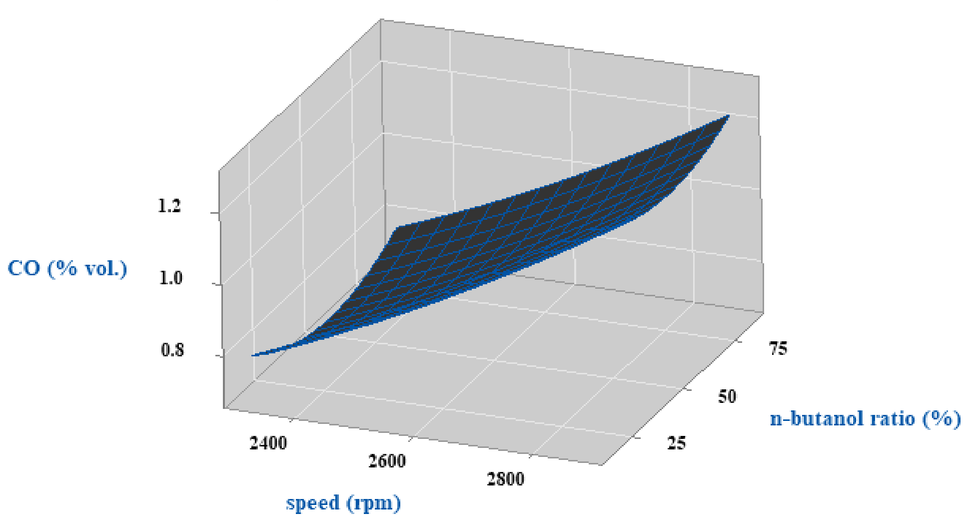

Figure 7. CO vs engine speed and n-butanol ratio surface plot

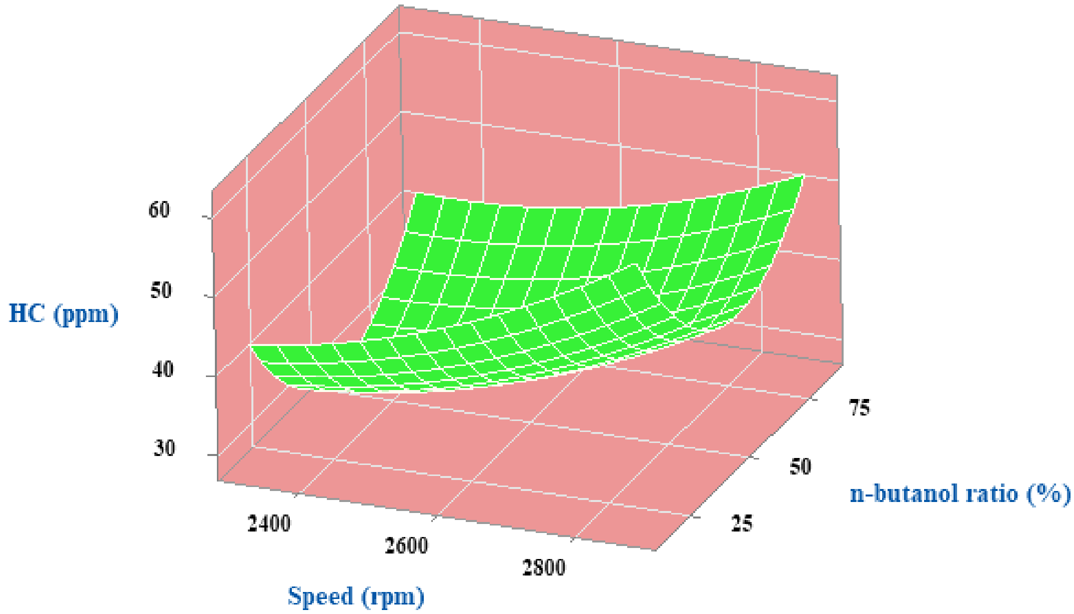

Figure 8: HC vs engine speed and n-butanol ratio surface plot

3.4 Response Surface Methodology Optimization

Using computational optimization with statistical software, the study focused on optimizing combinations of the seven response variables in the context of an RCCI engine mode. The primary goal was to enhance engine performance while maintaining emissions at the lowest possible levels. During the numerical optimization, the criteria were set to maximize BP and BT, while reducing BSFC, CO, CO_2, HC, and NOx. Table 8 illustrates the optimization setup, which is the adjusted values, to their lower and upper limits, of the parameters according to the model. Using the RSM optimizer, the optimal operating conditions were found to be a 2557 engine speed and 47% n-butanol ratio. Under these conditions, the best response achieved was a BT of 14.86 Nm, a BP of 4.04 kW, a BSFC of 0.379 kg/kWh, and CO_2, Co, NOx and HC emissions of 4.63 %vol., 0.87 %vol, 102 ppm, and 32 ppm, respectively. The RSM findings indicate that the performance and exhaust emissions parameters were significantly influenced by engine speed and n-butanol.

Table 8: The parameters setup for optimization

Response	Lower limit	Upper limit	Goal
Brake torque (Nm)	14.01	14.85	Maximize
Brake power (kW)	3.78	4.30	Maximize
Brake specific fuel consumption (kg/Kwh)	0.34	0.40	Minimize
Nitrogen oxides (ppm)	74.00	175.00	Minimize
Carbon dioxide (%vol.)	4.40	5.70	Minimize
Carbon monoxide (%vol.)	0.715	1.158	Minimize
Hydrocarbons (ppm)	28.00	51.00	Minimize

4. Conclusions

This study focused on how variations in engine speed and gasoline-n-butanol blend affect an RCCI engine mode. The modified CI engine to the RCCI engine was successfully operated under a various fuel, using biodiesel blend as HRF and gasoline/n-butanol blend as LRF. The experimental design, along with the RSM, was highly beneficial in identifying the values of the significant input variables that affect performance and emissions characteristics in the RCCI engine. The approach used significantly reduced the time required to achieve desired outcomes by minimizing the number of experiments needed.

Quadratic models were developed using the experimental data and the RSM was applied to predict BT, BP, BSFC, CO_2, CO, NOx, and HC with confidence levels, by varying the input variables. The R^2 values for BT, BP, BSFC, CO_2, CO, NOx, and HC are respectively, 97.98, 98.39, 98.62, 97.95, 98.89, 99.66 and 97.14%, all of which are close to 1, suggesting the good predictive ability of the model. The ANOVA analysis revealed that speed had more influence on BP, BSFC, CO_2, CO, NOx, and HC than the gasoline-n-butanol blend, while BT was more influenced by the gasoline-n-butanol blend. Generally, the optimum operating parameters for the current study are engine speed of 2557 rpm and 47 % n-butanol ratio.

Future investigations are suggested to concentrate on broadening the optimization framework to encompass additional intricate variables, including ignition delay, combustion duration, and exhaust gas recirculation rates, in order to gain a deeper insight into the combustion characteristics of RCCI engines. The integration of alternative low-reactivity fuels such as methanol or dimethyl ether, in conjunction with various biodiesel blends, has the potential to further improve emission control and thermal efficiency. Moreover, studies on long-term engine durability and deposit formation can be undertaken to evaluate the feasibility of optimized RCCI operation.

Acknowledgements: The authors express their gratitude to Adama Science and Techology University for financial support (Grant No. ASTU/SP-R/223/23) and to the Center of Excellence of Jimma Institute of Technology (JiT) for providing access to research facilities.

List of acronyms

AC	Alternating current
ANOVA	Analysis of variance
BP	Brake power
BSFC	Brake-specific fuel consumption
BT	Brake torque
CCD	Central composite design
CI	Compression engine
CO	Carbon monoxide
CO_2	Carbon dioxide
DOE	Design of experiment
EGA	Exhaust gas analyzer
HC	Hydrocarbon
HCCI	Homogeneous charge compression ignition
HRF	High reactivity fuel
LRF	Low reactivity fuel
NOx	Nitrogen oxides
PCCI	Premixed charge compression ignition
PI	Port injection
PM	Particulate matter
RCCI	Reactivity-controlled compression ignition

Reference

Chaudhari, V. D., & Deshmukh, D. (2019). Challenges in charge preparation and combustion in homogeneous charge compression ignition engines with biodiesel: A review. *Energy Reports*, 5, 960–968.

Deb, P., Singh, D., Kumar, M., & Paul, A. (2025). Effect of high reactive fuel injection advancement and hydrogen-biodiesel premix ratio on combustion, performance and emission of a CI engine under RCCI mode. *Fuel*, 382, 133710.

Elbanna, A.M., Xiaobei, C., Can, Y., Elkelawy, M., Alm-Eldin Bastawissi, H., & Panchal, H. (2022). Fuel reactivity controlled compression ignition engine and potential strategies to extend the engine operating range: A comprehensive review. *Energy Conversion and Management: X*, 13, 100133.

Elumalai, R., & Ravi, K. (2022). Strategy to reduce carbon emissions by adopting ammonia–Algal biodiesel in RCCI engine and optimize the fuel concoction using RSM methodology. *International Journal of Hydrogen Energy*, 47(94), 39701–39718.

Fırat, M., Altun, Ş., Okcu, M., & Varol, Y. (2022). Comparison of ethanol/diesel fuel dual direct injection (DI2) strategy with reactivity controlled compression ignition (RCCI) in a diesel research engine. *Energy*, 255, 124556.

Ganesan, N., Masimalai, S., Ekambaram, P., & Selvaraju, K. (2020). Experimental Assessment of Effects of n-Butanol on Performance, Emission, and Combustion Characteristics of Mahua Oil Fueled Reactivity Controlled Compression Ignition (RCCI) Engine. *Emission Control Science and Technology*, 6(3), 345–357.

Ganesh, D., Ayyappan, P. R., & Murugan, R. (2019). Experimental investigation of iso-butanol/diesel reactivity controlled compression ignition combustion in a non-road diesel engine. *Applied Energy*, 242, 1307–1319.

Habtamu Deresso Disassa, Ancha, V. R., & Nallamothu, R. B. (2023a). Experimental study of triple fuel physiognomies on LDRCCI diesel engine combustion. *Results in Engineering*, 20(x), 101451.

Habtamu Deresso Disassa, Ancha, V. R., Nallamothu, R. B., & Balewgize Amare Zeru (2023b). Experimental study on the effect of speed and port-injected fuel blend ratio on a reactivity-control compression ignition (RCCI) engine performance. *Energy Conversion and Management: X*, 20, 100448.

Habtamu Deresso Disassa, Ancha, V. R., Nallamothu, R. B., Bisrat Yoseph, & Getachew Alemayehu (2024). Response Analysis of an Experimental Study on the Effect of Speed and Premixed Fuel Ratio on Performance and Emissions in RCCI Engine. *International Journal of Chemical Engineering*, 2024.

Hayyan, A., Alam, Z. Mirghani, M.E.S., Kabbashi, A.N., Hakimi, N.I.N., Siran, Y.M., & Tahiruddin, S. (2011). Reduction of high content of free fatty acid in sludge palm oil via acid catalyst for biodiesel production Author links open overlay panel. *Fuel Processing Technology*, 92(5), 920-924.

Jagankumar, K. R., Prakash, N., Prasad, C., Shridhar, V. A., Dinesh Singh, M., & Sathyamurthy, R. (2020). An experimental investigation on single cylinder RCCI engine fuelled with diesel/petrol. *Journal of Physics: Conference Series*, 1706(1).

Jatoth, R., Gugulothu, S. K., Sastry, G. R. K., & Surya, M. S. (2021). Statistical and experimental investigation of the influence of fuel injection strategies on gasoline/diesel RCCI combustion and emission characteristics in a diesel engine. *International Journal of Green Energy*, 18(12), 1229–1248.

Jia, Z., & Denbratt, I. (2018). Experimental investigation into the combustion characteristics of a methanol-Diesel heavy duty engine operated in RCCI mode. *Fue*l, 226, 745–753.

Jin, C., Geng, Z., Zhang, X., Ma, M., Ji, J., Wang, G., Guan, C., & Liu, H. (2019). Study on the Solubility between Diesel and Acetone–Butanol–Ethanol with or without Water. *Energy & Fuels*, 34(2), 1166–1176.

Kakoee, A., Bakhshan, Y., Aval, S. M., & Gharehghani, A. (2018). An improvement of a lean burning condition of natural gas/diesel RCCI engine with a pre-chamber by using hydrogen. *Energy Conversion and Management*, 166, 489–499.

Kumar, M., & Paul, A. (2023). Comparative evaluation of combustion, performance, exergy and emission characteristics in hydrogen-biodiesel dual fuel engine under RCCI mode. *Energy & Environment,* 35(7), 3418-3440.

Liu, J., Wang, L., Wang, P., Sun, P., Liu, H., Meng, Z., Zhang, L., & Ma, H. (2022). An overview of polyoxymethylene dimethyl ethers as alternative fuel for compression ignition engines. *Fuel*, 318, 123582.

Mahla, S. K., Goga, G., Cho, H. M., Dhir, A., & Chauhan, B. S. (2023). Separate effect of biodiesel, n-butanol, and biogas on performance and emission characteristics of diesel engine: a review. *Biomass Conversion and Biorefinery*, 13(1), 447–469.

Mali, S. D., Shah, P. R., & Shah, D. R. (2024). Assessing performance variability in a dual-fuel diesel engine using diesel and biogas: an experimental study across different compression ratios. *Engineering Research Express*, 6, 035550.

Manojkumar, N., Muthukumaran, C., & Sharmila, G. (2022). A comprehensive review on the application of response surface methodology for optimization of biodiesel production using different oil sources. *Journal of King Saud University - Engineering Sciences*, 34(3), 198–208.

Negasa Tesfaye Tefera, Nallamothu, R. B., Getachew Alemayehu Lakew, & Teshome Kumsa Kurse. (2025a). Optimization of biodiesel production from cottonseed oil using response surface methodology and artificial neural network techniques. *Scientific African*, 28, e02665.

Negasa Tesfaye Tefera, Nallamothu, R. B., & Getachew Alemayehu. (2025b). Analysis of RCCI engine characteristics with n-butanol / gasoline as low reactive fuel and biodiesel blend as high reactive fuel. *Scientific reports*, 15, 26023.

Okcu, M., Varol, Y., Altun, Ş., & Fırat, M. (2021). Effects of isopropanol-butanol-ethanol (IBE) on combustion characteristics of a RCCI engine fueled by biodiesel fuel. *Sustainable Energy Technologies and Assessments*, 47, 101443.

Ouchikh, S., Lounici, M. S., Loubar, K., Tarabet, L., & Tazerout, M. (2022). Effect of diesel injection strategy on performance and emissions of CH4/diesel dual-fuel engine. *Fuel*, 308, 121911.

Pedrozo, V. B., Wang, X., Guan, W., & Zhao, H. (2022). The effects of natural gas composition on conventional dual-fuel and reactivity-controlled compression ignition combustion in a heavy-duty diesel engine. *International Journal of Engine Research*, 23(3), 397–415.

Rajavel, P., Arthanarisamy, M., & Ramasamy, S. (2025). Hybrid optimization of engine performance and emission using RSM-ANN-GA framework to explore valorization potential of waste cooking oil with green synthesized heterogenous ZnO nanocatalyst. *Fuel*, 395, 135092.

Ramachandran, E., Krishnaiah, R., Perumal Venkatesan, E., Medapati, S. R., & Sekar, P. (2023). Experimental Investigation on the PCCI Engine Fueled by Algal Biodiesel Blend with CuO Nanocatalyst Additive and Optimization of Fuel Combination for Improved Performance and Reduced Emissions at Various Load Conditions by RSM Technique. *ACS Omega*, 8(8), 8019–8033.

Ramachandran, M., & Subramanyan, N. (2024). Study and Optimization of Ethanol (LRF) Juliflora Biodiesel (HRF) Fuelled RCCI Engine with and without EGR System. *Tehnicki Vjesnik*, 31(3), 784–791.

Saxena, M. R., & Maurya, R. K. (2020). Influence of direct injection timing and mass of port injected gasoline on unregulated and nano-particle emissions from RCCI engine. *Fuel*, 282, 118815.

Shim, E., Park, H., & Bae, C. (2020). Comparisons of advanced combustion technologies (HCCI, PCCI, and dual-fuel PCCI) on engine performance and emission characteristics in a heavy-duty diesel engine. *Fuel*, 262, 116436.

Singh, D., Sharma, D., Soni, S. L., Sharma, S., & Kumari, D. (2019). Chemical compositions, properties, and standards for different generation biodiesels: A review. *Fuel*, 253, 60–71.

Vijai, C., Babu, M.D., Babu, M.N., Sathiyamoorthi, R., Sathyanarayanan, S., Sathya, V., KamakshiPriya, K., & Habtamu Alemayehu. (2025). Optimizing combustion efficiency and emission reduction in low temperature combustion engines using biodiesel-nano additive alcohol blends: A review. *Results in Engineering*, 27, 106175.

Wang, H., Liu, D., Ma, T., Tong, L., Zheng, Z., & Yao, M. (2019). Thermal efficiency improvement of PODE/Gasoline dual-fuel RCCI high load operation with EGR and air dilution. *Applied Thermal Engineering*, 159, 113763.

Wang, X., Zhang, Q., Liu, F., Jin, Y., & Li, X. (2021a). Experimental investigation on n-butanol/methyl oleate dual fuel RCCI combustion in a single cylinder engine at high-load condition. *Scientific Reports*, 11(1), 24211.

Wategave, S. P., Banapurmath, N. R., Nivedhitha, K. S., Sajjan, A. M., Sawant, M. S., Badruddin, I., Kamangar, S., & Hosmath, R. S. (2025). Combustion and emission characteristics of RCCI engine fueled with hydrogen and karanja biodiesel renewable fuels. *International Journal of Hydrogen Energy*, 123, 184–193.

Yohannes Kefale Mangesha, Nallamothu, R. B., Ancha, V. R., & Negasa Tesfaye Tefera (2024). Optimization, Production, and characterization of cottonseed methyl ester based on Box-Behnken in response surface design and gas Chromatography-Mass spectrum analysis. *Energy Conversion and Management: X*, 23, 100619.

Zarrinkolah, M. T., & Hosseini, V. (2022). Detailed analysis of the effects of biodiesel fraction increase on the combustion stability and characteristics of a reactivity-controlled compression ignition diesel-biodiesel/natural gas engine. *Energies*, 15(3), 1094.

Zhang, Q., Xia, J., Wang, J., He, Z., Qian, Y., & Lu, X. (2023). Experimental investigation on spray and combustion characteristics of dual-fuel collision of biodiesel and n-butanol. *Fuel*, 340, 127613.

Zhao, W., Zhang, Y., Huang, G., He, Z., Qian, Y., & Lu, X. (2021). Experimental investigation on combustion and emission characteristics of butanol/biodiesel under blend fuel mode, dual fuel RCCI and ICCI modes. *Fuel*, 305, 121590.

Zheng, Z., Xia, M., Liu, H., Wang, X., & Yao, M. (2018). Experimental study on combustion and emissions of dual fuel RCCI mode fueled with biodiesel/n-butanol, biodiesel/2, 5-dimethylfuran and biodiesel/ethanol. *Energy*, 148, 824–838.